Climate Dynamics (2019) 53:521–532
https://doi.org/10.1007/s00382-018-4597-1

A network-based comparative study of extreme tropical and frontal storm rainfall over Japan

Ugur Ozturk[1,2,3] · **Nishant Malik**[4] · **Kevin Cheung**[5] · **Norbert Marwan**[2] · **Juergen Kurths**[2,6]

Received: 12 July 2018 / Accepted: 19 December 2018 / Published online: 9 January 2019

Abstract
Frequent and intense rainfall events demand innovative techniques to better predict the extreme rainfall dynamics. This task requires essentially the assessment of the basic types of atmospheric processes that trigger extreme rainfall, and then to examine the differences between those processes, which may help to identify key patterns to improve predictive algorithms. We employ tools from network theory to compare the spatial features of extreme rainfall over the Japanese archipelago and surrounding areas caused by two atmospheric processes: the Baiu front, which occurs mainly in June and July (JJ), and the tropical storms from August to November (ASON). We infer from complex networks of satellite-derived rainfall data, which are based on the nonlinear correlation measure of event synchronization. We compare the spatial scales involved in both systems and identify different regions which receive rainfall due to the large spatial scale of the Baiu and tropical storm systems. We observed that the spatial scales involved in the Baiu driven rainfall extremes, including the synoptic processes behind the frontal development, are larger than tropical storms, which even have long tracks during extratropical transitions. We further delineate regions of coherent rainfall during the two seasons based on network communities, identifying the horizontal (east–west) rainfall bands during JJ over the Japanese archipelago, while during ASON these bands align with the island arc of Japan.

Keywords Extreme rainfall · Baiu · Tropical storms · Event synchronization · Complex networks

1 Introduction

The climate of Japan ranges from subarctic in the north (warm summers and snowy winters) to subtropical in the west with humid summers, and moderate and rainy winters, while eastern Japan is a transition zone (see Fig. 1). The surrounding seas partly moderate the climate by increasing the humidity levels. The Asian monsoon system also influences Japan's climate, which brings cold northeasterly winds in winter and wet air from south-southwest in summer. The *Baiu front* (also known as the *Meiyu front* in Southeast Asia) and *tropical storms* together with extra-tropical lows and local convection cells deliver nearly 75% of the total annual precipitation over Japan (Kanae et al. 2004; Saito et al. 2010). Studying the dynamics of the extreme rainfall is essential not only for informing quantitative assessments of concomitant flood and landslide hazards, but also to interpret their temporal trends as proxies for atmospheric warming (Knutson et al. 2010; Malik et al. 2016).

As part of the Asian monsoonal system, the *Baiu season* starts in late May with a northward shift in the North Pacific subtropical high (NPSH) (Suda and Asakura 1955; Krishnan and Sugi 2001; Okada and Yamazaki 2012). The front forms in early May, when warm maritime tropical air masses intersect with cool polar maritime air (Matsumoto 1989). In the following months of June and July, the Baiu front moves northwards with a northward shift of the polar

✉ Ugur Ozturk
ugur.oeztuerk@gfz-potsdam.de

1 Institute of Earth and Environmental Sciences, University of Potsdam, Potsdam, Germany

2 Potsdam Institute for Climate Impact Research, PIK, Potsdam, Germany

3 Helmholtz Centre Potsdam, GFZ German Research Centre for Geosciences, Potsdam, Germany

4 School of Mathematical Sciences, Rochester Institute of Technology, Rochester, USA

5 Department of Environmental Sciences, Macquarie University, Sydney, Australia

6 Department of Physics, Humboldt University, Berlin, Germany

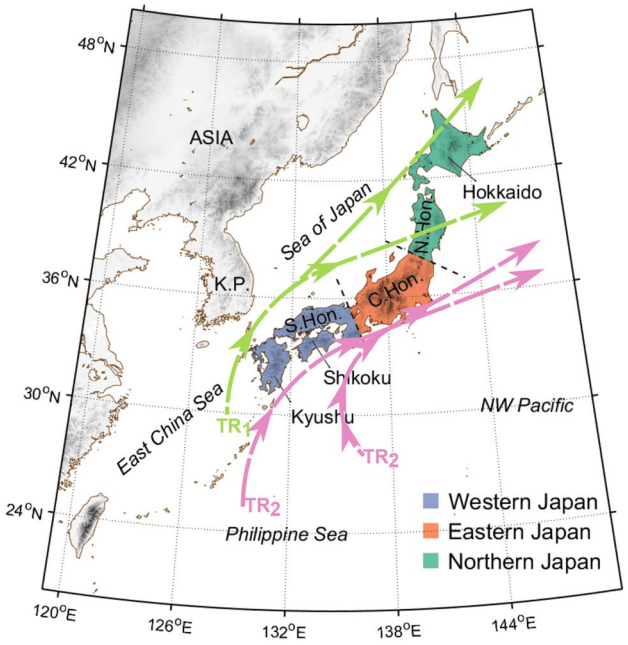

Fig. 1 Divisions of the four main islands of Japan into three subregions based on climatic characteristics by the Japan Meteorological Agency (JMA). TR_1 and TR_2 are the generalized typhoon tracks around Japan (Grossman and Zaiki 2009; Grossman et al. 2015). K.P. is the Korean Peninsula; S. Hon., C. Hon., and N. Hon. stands for Southern, Central, and Northern Honshu, respectively. Gray shading highlights the topography of up to 3500 m altitude

and subtropical jets, while the moisture is pushed eastwards onto Japan, leading to persistent and heavy quasi-stationary rainfall (Sampe and Xie 2010; Okada and Yamazaki 2012). During this period, mesoscale convective systems and/or mesoscale convective complexes cause significant downpours over spatial extents of 10^2 to 10^5 km^2. An abrupt northward migration of the subtropical jet over East Asia and a northward advance of the NPSH over the northwestern Pacific ends the Baiu season in late July (Ninomiya and Muraki 1986), unlike the Indian monsoon that continues until September or October (Stolbova et al. 2016). The end of the Baiu season is related to the northeast propagation of Rossby waves and southern convective activity (Enomoto et al. 2003; Okada and Yamazaki 2012). This eastward moisture flow at around 35°N (from 110°E to 150°E) is unique in the northern hemisphere and is held responsible for the extreme rainfall in Japan in early June to late July (Fukui 1970; Ninomiya 1984). Except for Hokkaido (northernmost main island), most of Japan experiences Baiu-derived heavy rainfall, which is most pronounced in Kyushu (the southernmost main island), which receives nearly half of its rainfall from June to July (Fig. 2a, c) (Matsumoto 1989).

A *tropical storm* is a rotating system (counterclockwise in the Northern Hemisphere) around its center (eye) characterized by thunderstorms and strong winds. Tropical storms are formed over large tropical water bodies, where evaporation boosts their energy. They can reach daily forward speeds (eye of the storm) of up to 500 km and make landfalls over large areas. For example, the Typhoon *Tip* (1979), the largest recorded tropical storm, was about 2000 km in diameter (Dunnavan and Diercks 1980). Similar to the Baiu front system, tropical storms have connections to the Asian monsoon system in the northwestern Pacific, while the Madden–Julian Oscillation modulates tropical storm activity over intraseasonal timescales by providing a favorable environment (Maloney and Hartmann 2001; Nakazawa 2006; Heistermann et al. 2013). Tropical storms bring heavy rainfall to Japan from May to November and their activity peaks around August and September (≥ 5/year). Tropical storms that travel to Japan mainly originate in the central-western Pacific. Tropical cyclones move westwards towards the Philippines or Taiwan before veering north to Japan and then proceeding to the east once more in mature stages (Fig. 1). They usually follow two generalized paths around Japan: the first group (TR_1) passes from the west of Kyushu towards the Sea of Japan, the second group (TR_2) approaches Kyushu or Shikoku from the east (NW Pacific or the Philippine Sea) (Grossman et al. 2015). About 80 tropical storms followed TR_1 in ASON between 1950 and 2016 according to the Japanese Meteorological Agency (JMA), whereas more than 200 approached Japan following TR_2. In later stages, the TR_1 bears either to northern Honshu ($\sim$ 55) or follows the way towards to Hokkaido ($\sim$ 25). Nearly all the TR_2 storms pass by the eastern shores of central Honshu (Eastern Japan) and bears to the east to the open ocean (Grossman and Zaiki 2009; Grossman et al. 2015). Tropical storms lose power in higher latitudes, when they encounter cold air masses and large vertical wind shear. However, they bring more than half of its annual rain to northern Japan (Fig. 2b), though the most intense rains occur around Kyushu (see Fig. 2d, f). Most tropical storms pass over Japan from the southwest to the northeast, which also leaves a footprint in the rainfall rates along this line (see Fig. 2d). Rainfall systems of tropical storms are classified into inner, outer and delta-shaped rain shields (Shimazu 1998). Inner rain shields (within 150–250 km of the eye) are present in all tropical storms, usually around the northeast and/or southeast of the eye (Ozturk et al. 2018). The outer rain shields exist only occasionally and extend towards northwest ($\sim$ 80%) or southwest ($\sim$ 20%) (Shimazu 1998). In some particular cases, the shape of the outer rain shields is transformed to a delta at the north of the eye when tropical storms approach mid-latitudes, these delta-shaped formations then rotate around the eye at $\sim$ 10°/h ($\sim$ 25–45 km/h) (Shimazu 1998). Tropical storms in the Northwest Pacific have shifted west towards South Korea with rising temperatures since the middle of the last

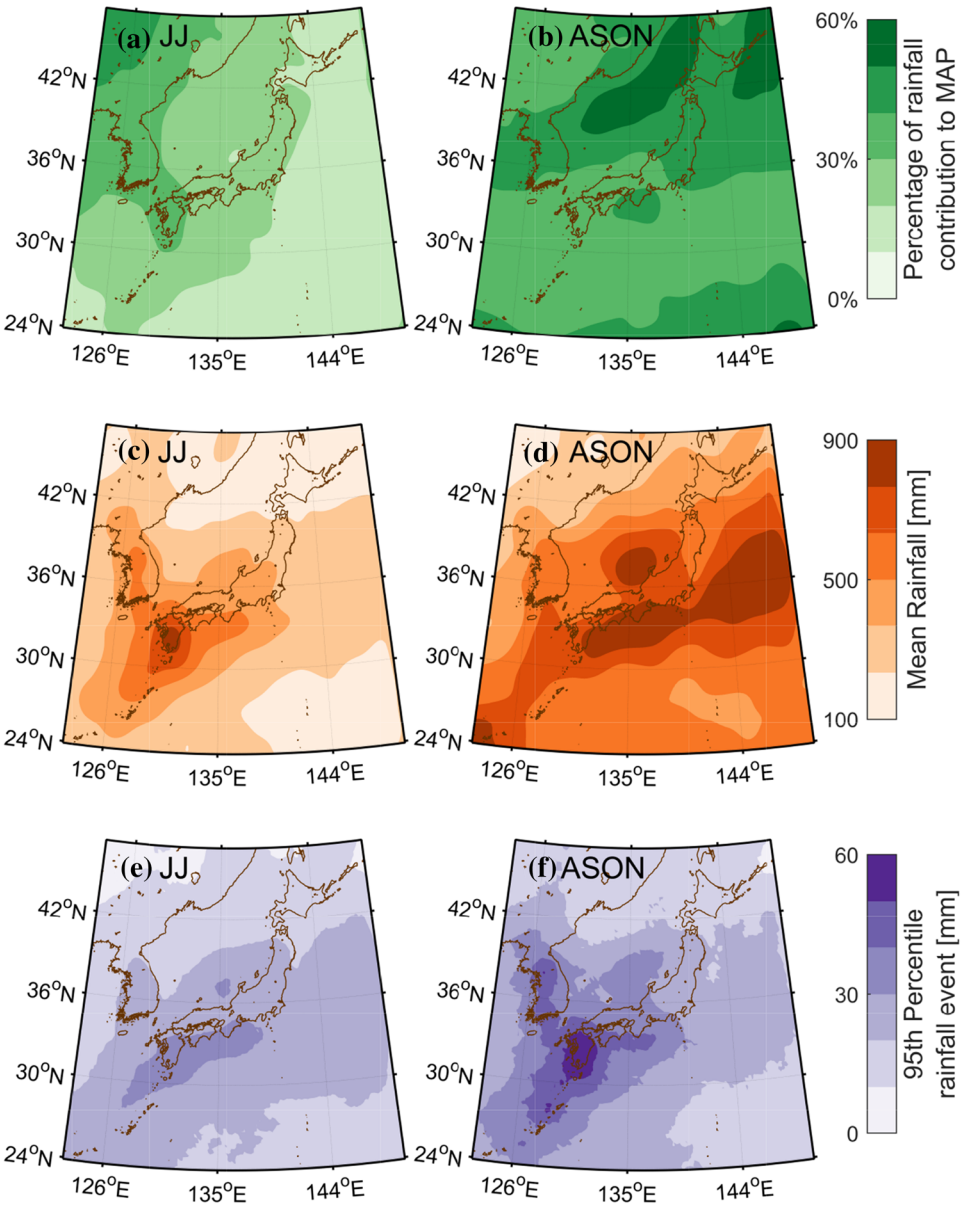

Fig. 2 Rainfall distributions in the study area. **a**, **b** Percentage of contribution to the mean annual precipitation (MAP, 1998–2015) from JJ (ASON) season. **c**, **d** Cumulative rainfall in JJ (ASON). **e**, **f** 95th percentile of rainfall intensities for the study periods

century (Webster 2005; Wu et al. 2005; Kim et al. 2006). Consequently, the number of tropical storms that make landfall in Japan has increased (Murakami et al. 2011; Manda et al. 2014).

Extreme rainfall events are expected to further increase in Japan during warm summer months, as projected by the 5th Assessment Report of the Intergovernmental Panel for Climate Change (IPCC) (Hartmann et al. 2013; Manda et al. 2014). Extent of this shift in the frequency of extreme events is likely to be more severe at locations, where the mean annual rainfall is high. Frequent short lasting rainstorms (> 1 day) with a high intensity may lead to an increase on the damage due to rainfall linked concomitant hazards, such as landslides and flash floods (Westra et al. 2014). Hence it is essential to study the spatial dynamics of the extreme rainfall.

Complex interactions between several variables, such as atmospheric pressure, humidity, temperature, wind, and topography, control the spatial dynamics of rainfall. This nonlinear interplay can complicate studying the climate system. Complex networks practically facilitate climate data, such as rainfall data that consists of spatial and temporal components, and helps inferring topological properties of the rainfall (Tsonis et al. 2006; Donges et al. 2009; Rheinwalt et al. 2012; Stolbova et al. 2014). The application of the complex networks theory to the analysis of spatiotemporal rainfall data has advanced our understanding of the various rain generating atmospheric processes (Malik et al.

2012; Boers et al. 2014; Agarwal et al. 2018b; Wolf et al. 2019). For example, frontal systems seem to control the extreme rainfall over the subtropics (Boers et al. 2014), and inter-seasonal oscillations in the extreme rainfall follow a spatial pattern during the Indian Summer Monsoon (Malik et al. 2012). Extreme rainfall over Japan and adjoining seas exhibit complex spatial and temporal patterns, and a complex network theory-based analysis of these patterns can augment our present knowledge of the extreme rainfall triggering atmospheric systems. Furthermore, identifying the contrasting features of tropical storms and the Baiu-linked frontal storms may provide additional insights into the key patterns that separate these two major atmospheric systems. Such patterns are particularly important when forecasting extreme rainfall events that are triggered by different atmospheric systems (Boers et al. 2014).

In this work, we carry out a comparative analysis of the spatial patterns of extreme rainfall driven by the Baiu front and tropical storms. Although it has been well-known that both weather systems are highly multi-scale in terms of their convective structures, traditionally they are analysed separately mostly by synoptic and mesoscale analysis. For the Baiu front, analysis usually was done on the frontal development, contribution from the Baiu trough, local circulation and embedded mesoscale convective systems in the front (Chen 2002). For tropical storms, the focus is usually on the eyewall structure (where the most intense rainfall is found), the outer rainbands, and interactions with mid-latitude systems during extratropical transition. Our primary aim here is to identify various contrasting features of the rainfall field during the Baiu and tropical storm seasons by a unified analysis framework. For this analysis, we employ quantitative tools from network science. In recent years, the analysis of extreme rainfall using methods of network science has provided substantial new insights into processes underlying extreme rainfall events (Agarwal et al. 2018b; Stolbova et al. 2014; Rheinwalt et al. 2012), in particular, during the Indian summer monsoon (Malik et al. 2012) or the South American monsoon (Boers et al. 2014). We adopt here the same techniques as used in the above works. However, these techniques are not yet employed in comparative studies of different rain generating phenomena over a region.

2 Data

In this study we employ satellite-derived daily (1998–2015) rainfall estimates from the Tropical Rainfall Measuring Mission (TRMM 3B42V7), which has a 0.25° spatial resolution (TRMM 2011). We split the data into two parts, the Baiu frontal storm season from June 1 to July 31 (JJ), and the tropical storm season from August 1 to November 30 (ASON) (Matsumoto 1989; Krishnan and Sugi 2001). We defined the rainfall above the ρth percentile ($\rho = 90\%$ or 95%) as extremes (Fig. 2e, f), where these are common thresholds in meteorological studies (Imaizumi et al. 2015; Castellano and DeGaetano 2016).

3 Methods

In this section, we introduce the mathematical tools used in the analysis. First, we describe the nonlinear correlation measure known as event synchronization and then follow with a brief description of network construction technique and network measures used in the study. Moreover, we discuss the connections between different network measures and meteorological processes.

3.1 Event synchronization

Event synchronization (ES) is a non-linear correlation measure for a time series with well-defined events (Quiroga et al. 2002; Malik et al. 2010; Agarwal et al. 2017). For example, in a rainfall time series events can be defined using different thresholds in terms of the rainfall amounts. We define extreme rainfall events in each time series based on a peak-over-threshold method that sets all events above ρth percentile as extremes (Lind et al. 2016). Note that the ρth percentile is determined for each time series independently. To measure the ES between two event time series, first, we compute time t_l^i at which an event l occurs at grid i, $l = 1, 2, 3, \ldots s_i$, where s_i is the total number of extreme events in the time series that occur over grid i. Two events occurring over grid points i and j are considered synchronized if these events occur within a time-period T_{lm}^{ij}, where it is defined as follows:

$$T_{lm}^{ij} = \frac{\min\left\{t_l^i - t_{l-1}^i, t_{l+1}^i - t_l^i, t_m^j - t_{m-1}^j, t_{m+1}^j - t_m^j\right\}}{2}, \tag{1}$$

where T_{lm}^{ij} is the shortest interval between the preceding and the successive events, and it is adaptive, i.e., it varies with changing frequency of events.

Next, we calculate $c(i|j)$, the number of synchronized events appearing at grid i after they appeared at j. $c(i|j)$ is calculated as,

$$c(i|j) = \sum_{l=1}^{s_i} \sum_{m=1}^{s_j} J_{ij}, \tag{2}$$

where,

$$J_{ij} = \begin{cases} 1 & \text{if } 0 < t_l^i - t_m^j \\ \frac{1}{2} & \text{if } t_l^i - t_m^j = 0 \\ 0 & \text{else.} \end{cases} \tag{3}$$

Similarly, $c(j|i)$ can be calculated. Then, the strength of ES between grid i and j is given by Q_{ij},

$$Q_{ij} = \frac{c_{ij} + c_{ji}}{\sqrt{(s_i - 2) \cdot (s_j - 2)}}. \tag{4}$$

Q_{ij} is a symmetric quantity i.e., $Q_{ij} = Q_{ji}$ and where $0 \leqslant Q_{ij} \leqslant 1$, $Q_{ij} = 1$ implies complete synchronization between grid i and j.

For our analysis, we calculate a Q_{ij} matrix for the TRMM data, which consists of daily rainfall recorded over a spatial grid, extending from 23.875°N to 47.125°N latitudinally and 122.875°E to 149.625°E longitudinally. Each rectangular cell within the spatial grid has a spatial resolution of 0.25°, i.e., we have 10152 grid cells covering the whole study region. Hence, the dimensions of the Q_{ij} matrix are 10152×10152. Let us refer to the ES matrix calculated using the ρ percentile threshold for defining an extreme event as Q^{ρ}_{ij}.

To construct a network from the Q^{ρ}_{ij} matrix, we assume that the spatial grid points of the TRMM data are nodes of a network and edges between these nodes exists only if Q^{ρ}_{ij} is above a certain threshold. As the largest values in Q^{ρ}_{ij} are the outcomes of the most correlated atmospheric features, we assume grids (nodes) above the γ percentile of Q^{ρ}_{ij} values are connected. For example, when $\gamma = 95\%$, the edges (links) are between nodes with the top 5% of Q^{ρ}_{ij} values. An undirected network is represented by a binary square matrix, known as the adjacency matrix $A^{\rho\gamma}_{ij}$. Here, we can obtain such a matrix as follows:

$$A^{\rho\gamma}_{ij} = \begin{cases} 1 & \text{if } Q^{\rho}_{ij} \geq \alpha(\gamma) \\ 0 & \text{if } Q^{\rho}_{ij} < \alpha(\gamma), \end{cases} \tag{5}$$

where $\alpha(\gamma)$ is the corresponding threshold on Q^{ρ}_{ij} for a given γ. If there exists an edge between grid i and j, then $A^{\rho\gamma}_{ij} = 1$, else $A^{\rho\gamma}_{ij} = 0$.

3.2 Network measures and properties

A complex network consist of nodes, which are the geographical coordinates of the TRMM time series in this study, and edges, which identify the connected nodes, decoded in the adjacency matrix $A^{\rho\gamma}_{ij}$. The physical length of edges is a measure of the spatial scales involved in the rain producing atmospheric processes (Malik et al. 2012). We analyze the distribution of (azimuthal) length of edges $\mathscr{L}$ (Schieber et al. 2017) to quantify the global differences between spatial scales involved in the Baiu front and tropical storms driven rainfall. To identify these differences at finer scales, we use the mean edge length (azimuthal) $\mathscr{L}_{mean}$ of all the edges incident on a node.

Centrality measures indicate the importance of nodes in a complex network. We first investigate the degree centrality k for both Baiu and tropical storm seasons. High k nodes are the central nodes of a network. They are measured by counting the number of edges incident upon the node (Newman 2010). The k of the node i is,

$$k_i = \sum_{j=1}^{n} A_{ij}, \tag{6}$$

where n is the total number of nodes in a network, and A_{ij} indexes whether there is an edge between node i and j. Highly connected regions will have large k values, where these regions are the ones where rainfall is an outcome of large-scale spatial atmospheric processes (Tsonis and Swanson 2008; Malik et al. 2012). For example, giant topographic barriers tend to disintegrate large-scale spatial atmospheric processes and hence one observes low degree centrality across topographic barriers (Malik et al. 2012; Stolbova et al. 2014). Regions with low k values are the ones where rainfall is an outcome of isolated and small-spatial atmospheric processes (Boers et al. 2014; Stolbova et al. 2014).

Another critical centrality measure is the closeness χ; it is the normalized total sum of the shortest paths between a node and all other nodes in a network (Sabidussi 1966; Newman 2010). Thus, it measures the average network distance between a node and its neighbors. The χ of the node i is given by,

$$\chi_i = \frac{1}{\sum_{j=1}^{n} d_{ij}}, \tag{7}$$

where d_{ij} stands for the distance between nodes i and j. Any perturbation introduced at the nodes (regions) with the highest χ will disperse over the network at a faster rate (Malik et al. 2012). Hence, it locates the nodes, where the information flow (in the context of this study, rainfall dynamics) is the fastest. Regions with high χ will significantly impact upon meteorological processes, including rain producing systems. High χ corresponds to a rainfall system, which is effective over a large area (e.g., Indian summer monsoon), while low χ indicates locally effective rainfall with minor movement (e.g., short lived frontal systems).

We also study one of the most fundamental structural property of real-world networks, the clustering coefficient C (Watts and Strogatz 1998). Mathematically, it measures the frequency of triangles in a network, i.e., the number of 3-vertex cliques (triangles) in which all three nodes are connected. The C of the node i,

$$C_i = \frac{\sum_i A_{ij} \cdot A_{ih} \cdot A_{jh}}{k_i}, \tag{8}$$

where A_{ij}, A_{ih}, and A_{jh} indicate whether there is an edge between node i and j, i and h, j and h, respectively. The local clustering coefficient measures the ratio of links connecting the direct neighbours of a particular node to the number of all possible links between them (Jha et al. 2015), and it is a characteristic of the spatial continuity of the rainfall field. High C indicates an atmospheric system that brings rainfall to a large region at once (e.g., warm frontal precipitation in a developing cyclone system), while low C means scattered rainfalls without any physical connection between the local rainfall events (e.g., small-scale, isolated moist convections). Thus, the local clustering coefficient is able to distinguish rainfall generated from large-scale systems or in a smoother form (e.g., stratiform rain) versus mesoscale and convective-scale rainfall.

Centrality measures are subject to embedding biases, for example, borders of the study site remove edges that may exist with the area outside of the study site. We have corrected such boundary effects in the centrality measures using the numerical solution proposed by Rheinwalt et al. (2012). The algorithm estimates the boundary effect iteratively based on the existence of edges in spatially embedded random networks that mimic the edge length (azimuthal) distribution of the original network.

We complete the analysis by finding communities F that best partition the networks for the Baiu front and tropical storms. Communities in a network represent groups of nodes that are highly connected within each group, but with weaker links among the groups (Fang et al. 2017). An analogue may be the traditional clustering analysis in statistics. There are many algorithms for identifying network communities (Arenas 2005; Fortunato and Hric 2016). We use an algorithm which involves the maximization of modularity, see Blondel et al. (2008) for details. Although modularity is commonly applied to explore the communities in network studies, it is not widely used in climate networks (Agarwal et al. 2018). We choose the algorithm by Blondel et al. (2008) particularly because of the high computation speed and accuracy. These communities are representative of coherent rainfall zones over the study area, i.e., the rainfall over these zones is more homogeneous, synchronized and have similar dynamical properties.

4 Results and discussion

Extreme rainfall is triggered by several weather systems, in addition to tropical or frontal systems, e.g., orographic downpours linked to low-level jets (Monaghan et al. 2010; Sato 2013) might also trigger extreme rainfall. Hence, we consider the following different combinations of the thresholds ρ and γ in our above-described method (Eq. 5): $(\rho, \gamma) = (90\%, 90\%), (95\%, 90\%), (90\%, 95\%)$ and $(95\%, 95\%)$. We try to minimize the bias in our event series due to the extremes that might have been triggered by the other rainfall systems by setting ρ as high as 90% or 95%. We will show only one case to conserve space in the figures with spatial maps of the region. However, we have checked that these results are not sensitive to the above choices of thresholds.

The distribution of the length of the edges $\mathscr{L}$ is shown in Fig. 3. We identify that $\mathscr{L}$ follows a good approximation of a gamma (Weibull) distribution in JJ (ASON). Both of these distributions are extensions of the exponential distribution and are frequently encountered in the modeling of extreme events. In contrast to JJ, it appears that rainfall events during ASON tend to cluster more towards specific length scales leading to a Weibull distribution (observe the higher peak values for ASON in Fig. 3a–d). Also, JJ has more spread out tails, i.e., *the spatial scales of extreme rainfall during JJ are longer compared to ASON* when $\gamma = 90\%$, including a larger mean length (note the difference in μ_{JJ} and μ_{ASON} values in Fig. 3).

This result may seem at first counter-intuitive because the spatial length scales of the rainfall field are bound to the forward speed and the size of the tropical storms during ASON, and when they travel long distances during the extratropical transition the rainfall field is expected to be connected over such long distances. This fact of longer mean edge lengths in JJ is linked to the Baiu front development, which starts over east China associated with the Baiu trough and extends all along western and eastern Japan (with possible interaction with other cyclonic systems) towards northwestern Pacific for about 3000 km (Laing and Evans 2015). Hence the Baiu linked events during JJ can occur over larger spatial scales than the tropical storm dependent events.

Spatially, the longest mean geographical lengths of edges $\mathscr{L}_{mean}$, exist over the Sea of Japan for the JJ season whereas, for the ASON season, parts of northern Japan and the northwest Pacific have longer mean geographical length of edges (see Fig. 4a–c). In Fig. 5a, b we observe a similar pattern for the degree centrality k as well (Eq. 6). The regions mentioned above are not those with the highest rainfall amounts, but the relatively drier regions during the JJ and ASON season (see Fig. 2). The Baiu front is a highly multi-scale phenomenon (Ninomiya and Akiyama 1992; Ninomiya and Shibagaki 2007). During such frontal developments in JJ, mid-level shortwaves from north China together with southwesterlies from lower latitudes create the Baiu trough over the northern Sea of Japan. However, when the frontal activity effects southern Japan, the heavy rainfall is often due to mesoscale convective systems embedded in the front, sometimes related to topographic effects over land. The mesoscale systems would reduce $\mathscr{L}_{mean}$ and k from the network perspective, because of the much-localized extreme rainfall (see western Japan in Figs. 4a, 5a). Both $\mathscr{L}_{mean}$ and k patterns match with the typical TR_1 and TR_2 tropical storm paths in

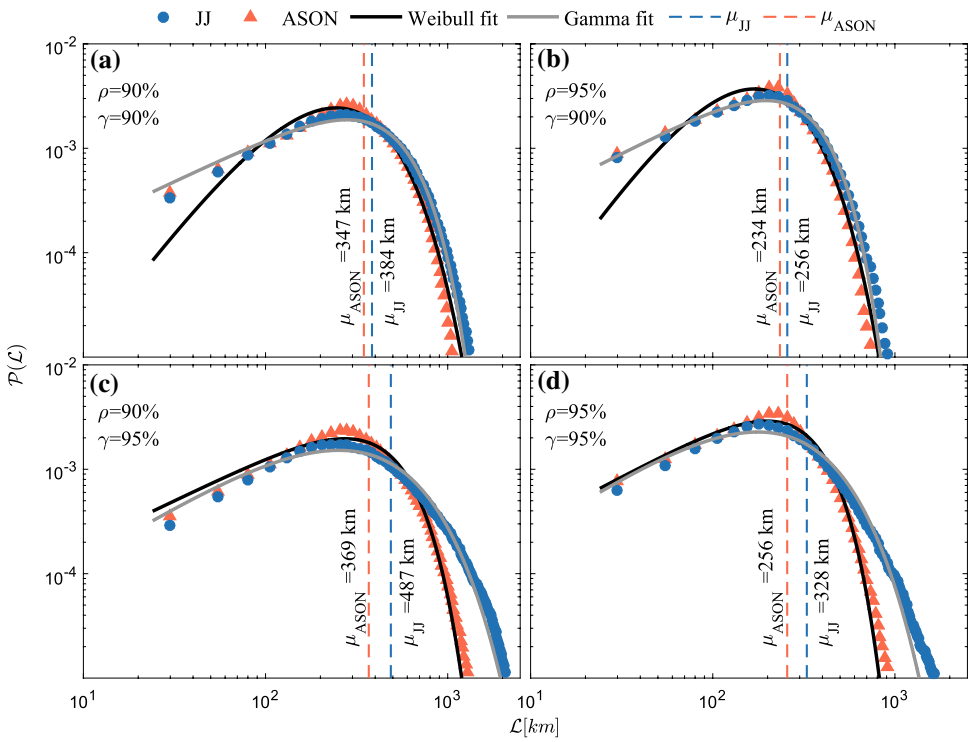

Fig. 3 Node distance (azimuthal) distribution of the rainfall networks and the fitted distributions (i.e. Weibull $f(x|\lambda,k) = \frac{k}{\lambda} \cdot (\frac{x}{\lambda})^{k-1} \cdot e^{-(x/\lambda)^k}$ and Gamma $f(x|\kappa,\theta) = \frac{1}{\theta^\kappa \cdot \Gamma(\kappa)} \cdot x^{\kappa-1} \cdot e^{\frac{-x}{\theta}}$). **a** The strength parameter Q_{ij} is derived from the rainfall extremes above $\rho = 90\%$ (Q^{90}), and γ allows 10% of the highest correlated nodes ($\gamma = 90\%$) to be connected in the network (A^{90}) ($\lambda = 433, k = 1.8, \kappa = 3.4, \theta = 103$). **b** $Q^{95} - A^{90}$ ($\lambda = 290, k = 1.9, \kappa = 3.6, \theta = 65$). **c** $Q^{90} - A^{95}$ ($\lambda = 416, k = 1.8, \kappa = 2.1, \theta = 235$). **d** $Q^{95} - A^{95}$ ($\lambda = 290, k = 1.9, \kappa = 2.2, \theta = 151$)

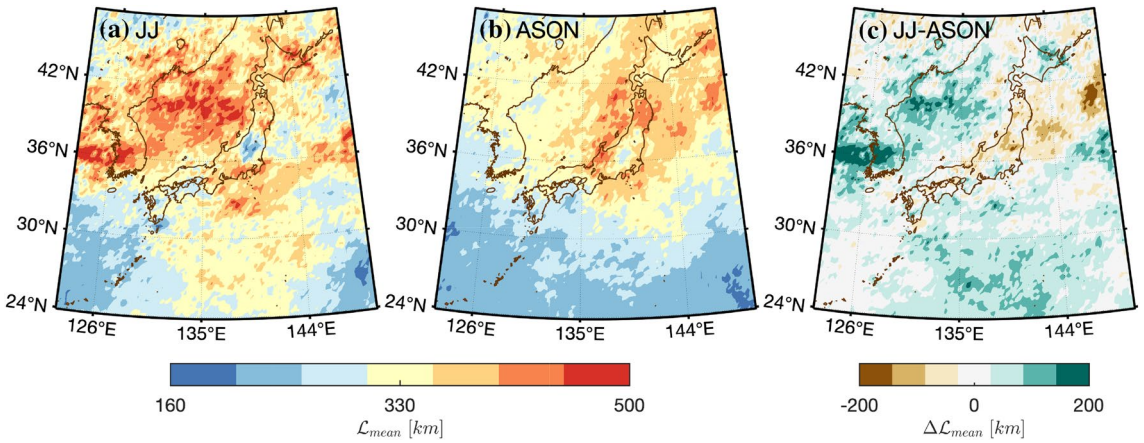

Fig. 4 Mean edge length $\mathscr{L}_{mean}$ for $Q^{90} - A^{95}$ in the periods **a** *JJ*, **b** *ASON*, and **c** their difference $\Delta\mathscr{L}_{mean} = \mathscr{L}_{mean}(JJ) - \mathscr{L}_{mean}(ASON)$

ASON, one south and another north of Honshu island. The tropical storm rainfall following these paths is revealed in these two network metrics. Hence, from these observations, we can infer that rainfall over the Sea of Japan during JJ, and northern Japan and the northwest Pacific during ASON is the outcome of the most extended spatial scale atmospheric processes that generate the extreme rainfall associated with the Baiu front and tropical storms.

Quite distinct from the mean edge length and degree centrality, all the regions with higher closeness χ (Eq. 7) are around the boundary of the studied region for the JJ season, but unlike $\mathscr{L}_{mean}$ and k, with lower values over the Sea of Japan, indicating that the processes that impact the JJ rainfall are larger than the area of study (Fig. 6). The JJ season receives rainfall due to the movement of the Baiu front, which is a massive spatial scale process and controlled by planetary-scale processes such as Rossby waves and accompanied Baiu trough development. Since χ emphasizes the pathways of extreme rainfall more (even when degree centrality is small), the pattern in Fig. 6a nicely indicates the northward movement of the Baiu front, shown by the yellow coloured area that extends from 30°N to 40°N on Japan and Sea of Japan. The regions with even higher closeness (red coloured) can be seen extending to the northern Sea of Japan

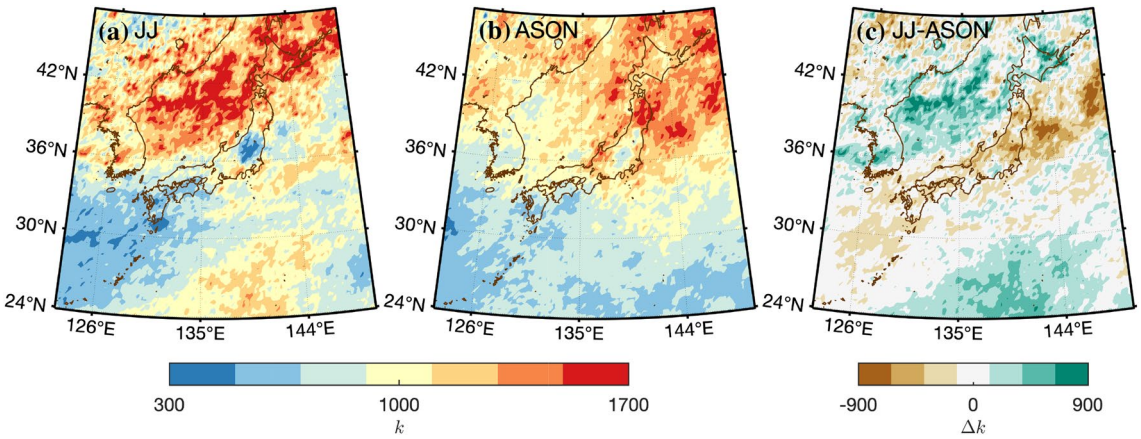

Fig. 5 Degree centrality k for $Q^{90} - A^{95}$ in the periods **a** *JJ*, **b** *ASON*, and **c** their difference $\Delta k = k(JJ) - k(ASON)$

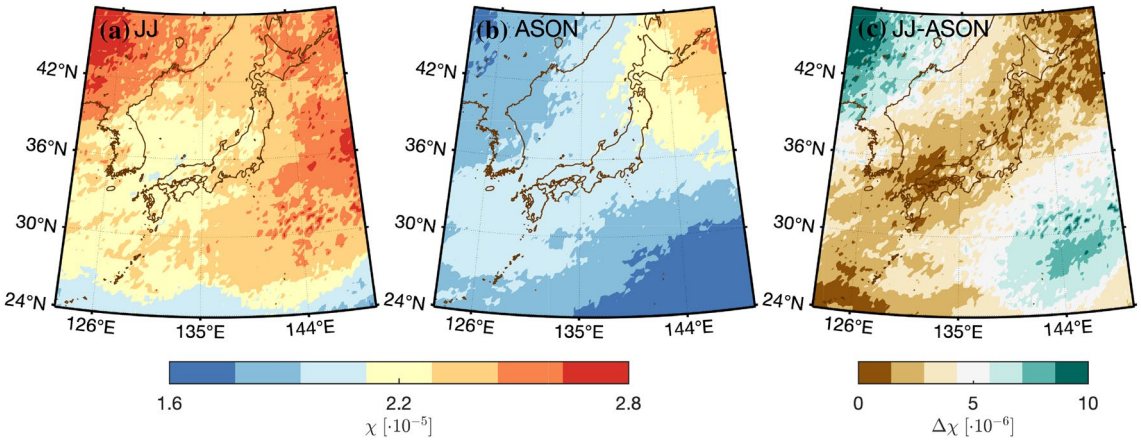

Fig. 6 Closeness centrality χ for $Q^{90} - A^{95}$ in the periods **a** *JJ*, **b** *ASON*, and **c** their difference $\Delta\chi = \chi(JJ) - \chi(ASON)$

and northwest Pacific, indicating the connection between Baiu rainfall and other synoptic systems in the vicinity. In contrast, for the ASON season, the higher χ regions lie along the Japanese archipelago, with most higher values observed over northern Japan. Tropical storms traveling along the Japanese archipelago cause the ASON rainfall (see TR_1 and TR_2 tracks of tropical storms in Fig. 1). Hence, ASON rainfall is mainly influenced by processes taking place over the Japanese archipelago, including the interaction with the topography of the region. Higher χ values during the JJ season indicates once again the larger scale of the Baiu frontal system compared to tropical storm systems during the ASON season. In Fig. 6c, we plot the difference between χ during JJ and ASON, where a diagonal pattern along the Japanese archipelago becomes even more evident.

The local clustering coefficient C (Eq. 8) measures the interconnections between network nodes (triangles of vertices), and C indicates the continuity of the rainfall fields in rainfall networks. Higher C means that the rainfall field is more homogeneous in space, whereas lower C refers to a spatially heterogeneous rainfall field. We do not observe a specific spatial pattern in C over the area of interest for JJ (see Fig. 7a). This is consistent with the fact that the extreme rainfall within the Baiu front is often from the mesoscale convective systems and they have highly variable locations. However, we do observe higher C over Eastern Japan (Central Honshu) in the case of ASON, which is the region with a very high topography, including the Japanese Alps. It, therefore, appears that tropical storms interact with the topography of the Japanese archipelago. Also, at the latitudes of Japan, tropical storms interact with the persistently large vertical wind shear in the region, which often results in typical rainfall patterns under the influence of westerly shear. This may be one of the reasons, other than the topography, of the higher clustering coefficient during ASON compared with JJ.

Next, we identify regions of coherent rainfall activity during the JJ and ASON seasons. For this purpose, we identify

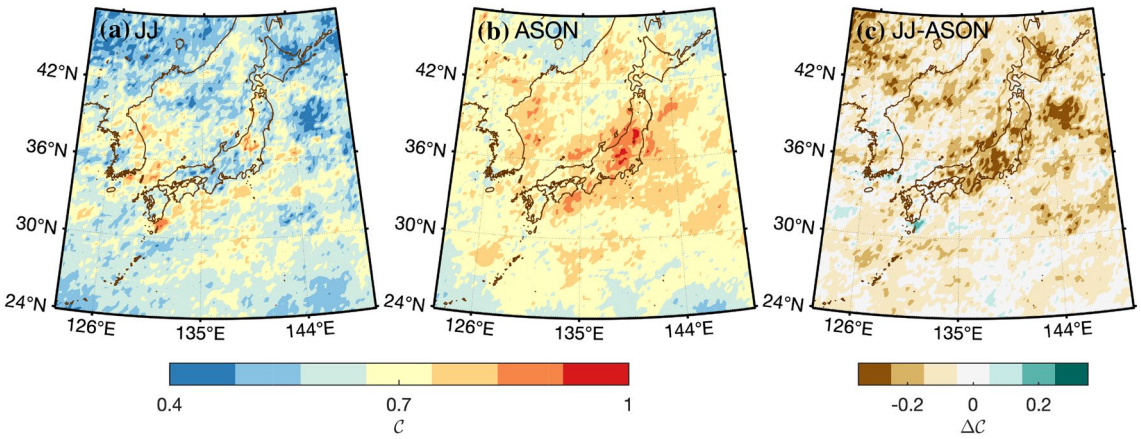

Fig. 7 Local clustering C for $Q^{90} - A^{95}$ in the periods **a** *JJ*, **b** *ASON*, and **c** their difference $\Delta C = C(JJ) - C(ASON)$

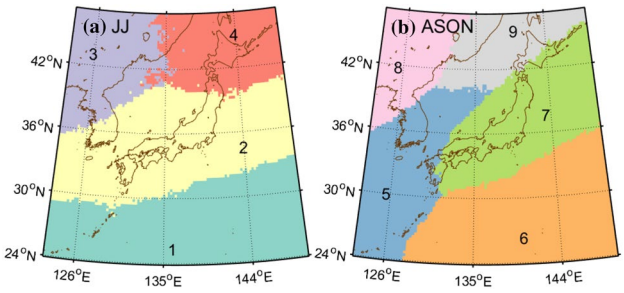

Fig. 8 Communities F for $Q^{90} - A^{95}$ in the periods **a** *JJ*, and **b** *ASON*

the community structure in the networks, i.e., we partition network nodes into different groups or communities. We use the modularity maximization method (Louvain method) to detect communities by iteratively optimizing the local communities up to a level that the global modularity can no longer be improved (Blondel et al. 2008). Communities represent highly interconnected parts of a network or functional modules within a network. In rainfall networks, communities can identify the regions of coherent rainfall activity; according to our definition of edges, which is based on event synchronization, they are the regions with more synchronized and homogenized rainfall.

We identified four communities for the JJ season by maximizing the modularity (see Fig. 8a). The communities in Fig. 8a appears to capture the fact that the Baiu front gradually moves northwards from the south of the area shown. Baiu fronts are typically heavily elongated, extending zonally (east–west) rather than meridionally (north–south), which is seen by the horizontally-extending community *2* that includes the highest rainfall regions. The northern most latitudes are divided into two communities, possibly due to the mechanisms involved at the end of the Baiu season, for example the northward advance of the NPSH over the northwestern Pacific (associated with community *4*). On the other hand, community *3* is associated more with monsoon development processes over East Asia. In the case of the ASON season, we obtain five communities (see Fig. 8b). Communities *6* and *7* appear to be due to the track TR_2 of the tropical storms, and communities *5* and *9* are due to the track TR_1 of the tropical storms. $\sim 2/3$ of the track TR_1 appear to converge towards northern Honshu and merge with community *7*, whereas the remaining $\sim 1/3$ represent community *9*, where tropical storms lose energy in such northern latitudes ($> 40°$N). Most of Japan appears to fall within one single coherent rainfall community during ASON (see community *7* in Fig. 8b), with only some parts of Hokkaido and southern Japan being outside of it. The area marked by the community *7* is emphasized also by high clustering in Fig. 7b, which we interpret as the large cloud systems being effective over the region concurrently and distinct topographic effect to rainfall is highlighted over the Japan Alps. Whereas, during the JJ there exist a clean division between northern (Hokkaido and North Honshu) and rest of Japan, where Baiu is active.

5 Conclusion

Spatially embedded climate networks have been recently adopted to uncover non-linear climatic processes over large spatial scales, such as the spatial distribution of extreme rainfall over the Indian subcontinent during the Indian Summer Monsoon (Malik et al. 2012; Stolbova et al. 2014), or the propagation of extreme rainfall over south America (Boers et al. 2014). This study is the first example in which complex networks are adopted to compare the spatial dynamics of two different atmospheric systems that commonly initiates extreme rainfall, the Baiu front, and tropical storms, which bring rainfall to Japan. We have employed tools from network science to analyse satellite-derived daily rainfall on

two disjointed seasons; JJ and ASON, for the analysis. The Baiu front is the main source of rainfall during JJ and tropical storms during ASON. Consistency of the Baiu season decreases the chance of biases due to tropical storms during JJ, which is reflected clearly in our results.

Complex network measures are able to effectively identify different areas where contrasting tropical storm tracks are effective using only TRMM rainfall estimates. Although the spatial dynamics of the Baiu frontal system was long studied, this study might be the first that numerically identifies the Baiu dominated region on Japan on a decadal time scale.

We have uncovered that spatial scales involved in rainfall caused by the Baiu season are longer ($\sim 10^3$ km) than rainfall produced by tropical storms, when the longest links are considered, and follow a gamma distribution. Tropical storms show a preference for moderate length scales in the range of 10^2 km and follow a Weibull distribution. The longer scales should be related to the fact that the Baiu front is a *nearly stationary weak baroclinic zone*, whereas the tropical storms are highly dynamic, closed low-level atmospheric circulations.

The longest length scale rainfall during the Baiu season seems to exist over the Sea of Japan, one of the driest regions during this period (versus Western Japan) associated with the shortwave from the Asia continent and southwesterlies from land. It appears that the Sea of Japan receives rainfall as a result of massive spatial activities of the atmosphere, which are responsible for generating the Baiu trough. During the tropical storm season, spatially massive storms bring rainfall over northern Japan along the two typical storm track types. These different scales of processes associated with Baiu front and tropical storms have been revealed from various network measures based on event synchronization, such as mean edge length $\mathscr{L}_{mean}$, degree k and closeness χ centralities. The first two measures indicate the more local characteristics of the extreme rainfall, while closeness centrality, by its definition, is able to indicate the pathway of development of extreme rainfall event and spatial relationships with other synoptic systems.

We suspect that the processes impacting upon the Baiu season are of a planetary scale, whereas local processes that are active around the Japanese archipelago influence the tropical storms, including the topography of different islands. We have further identified, based on network communities F, that during JJ there exist east-west bands of coherent rainfall over the study region. In contrast, bands of coherent rainfall form along the tracks for tropical storms during ASON season.

Acknowledgements We thank Ankit Agarwal, Aljoscha Rheinwalt and Bedartha Goswami for helping with some of the computations. We acknowledge Vera Ozturk for helping us in visualization. We also thank Kevin Fleming for proofreading the manuscript. Our research is funded by the Deutsche Forschungsgemeinschaft within the Research Training Group "Natural Hazards and Risks in a Changing World (NatRiskChange)" (DFG GRK 2043/1) at the University of Potsdam. Ugur Ozturk is partly funded by the Federal Ministry of Education and Research (BMBF) within the project CLIENT II-CaTeNA (FKZ 03G0878A). We are grateful to the Tropical Rainfall Measuring Mission (TRMM) for providing the data for this research (https://pmm.nasa.gov/data-access/downloads/trmm).

References

Agarwal A, Marwan N, Rathinasamy M, Merz B, Kurths J (2017) Multi-scale event synchronization analysis for unravelling climate processes: a wavelet-based approach. Nonlinear Process Geophys 24(4):599–611. https://doi.org/10.5194/npg-24-599-2017

Agarwal A, Marwan N, Maheswaran R, Merz B, Kurths J (2018a) Quantifying the roles of single stations within homogeneous regions using complex network analysis. J Hydrol 563:802–810. https://doi.org/10.1016/j.jhydrol.2018.06.050

Agarwal A, Marwan N, Rathinasamy M, Ozturk U, Merz B, Kurths J (2018b) Optimal design of hydrometric station networks based on complex network analysis. Hydrol Earth Syst Sci Discuss. https://doi.org/10.5194/hess-2018-113

Blondel VD, Guillaume JL, Lambiotte R, Lefebvre E (2008) Fast unfolding of communities in large networks. J Stat Mech Theory Exp 10:P10008. https://doi.org/10.1088/1742-5468/2008/10/P10008

Boers N, Bookhagen B, Barbosa HMJ, Marwan N, Kurths J, Marengo JA (2014a) Prediction of extreme floods in the eastern Central Andes based on a complex networks approach. Nat Commun 5:5199. https://doi.org/10.1038/ncomms6199

Boers N, Rheinwalt A, Bookhagen B, Barbosa HMJ, Marwan N, Marengo J, Kurths J (2014b) The South American rainfall dipole: a complexnetwork analysis of extreme events: BOERS ET AL. Geophys Res Lett 41(20):7397–7405. https://doi.org/10.1002/2014GL061829

Castellano CM, DeGaetano AT (2016) A multi-step approach for downscaling daily precipitation extremes from historical analogues: downscaling precipitation extremes from historical analogues. Int J Climatol 36(4):1797–1807. https://doi.org/10.1002/joc.4460

Chen GTJ (2002) Convection and local circulations under the influence of Meiyu front over Northern Taiwan. In: East Asia and Western Pacific meteorology and climate, world scientific series on Asia-Pacific Weather and Climate, vol 1. World Scientific Publishing Co, pp 275–292. https://doi.org/10.1142/9789812777744_0026

Donges JF, Zou Y, Marwan N, Kurths J (2009) Complex networks in climate dynamics. Eur Phys J Spec Top 174(1):157–179. https://doi.org/10.1140/epjst/e2009-01098-2

Duch J, Arenas A (2005) Community detection in complex networks using extremal optimization. Phys Rev E .https://doi.org/10.1103/PhysRevE.72.027104

Dunnavan GM, Diercks JW (1980) An analysis of super typhoon tip (October 1979). Mon Weather Rev 108(11):1915–1923. https://doi.org/10.1175/1520-0493(1980)108<1915:AAOSTT>2.0.CO;2

Enomoto T, Hoskins BJ, Matsuda Y (2003) The formation mechanism of the Bonin high in August. Q J R Meteorol Soc 129(587):157–178. https://doi.org/10.1256/qj.01.211

Fang K, Sivakumar B, Woldemeskel FM (2017) Complex networks, community structure, and catchment classification in a large-scale river basin. J Hydrol 545:478–493. https://doi.org/10.1016/j.jhydrol.2016.11.056

Fortunato S, Hric D (2016) Community detection in networks: a user guide. Phys Rep 659:1–44. https://doi.org/10.1016/j.physrep.2016.09.002

Fukui E (1970) Distribution of extraordinarily heavy rainfalls in Japan. Geogr Rev Jpn 43(10):581–593. https://doi.org/10.4157/grj.43.581

Grossman M, Zaiki M (2009) Reconstructing typhoons in Japan in the 1880s from documentary records. Weather 64(12):315–322. https://doi.org/10.1002/wea.401

Grossman MJ, Zaiki M, Nagata R (2015) Interannual and interdecadal variations in typhoon tracks around Japan: interannual and interdecadal variations in typhoon tracks around Japan. Int J Climatol 35(9):2514–2527. https://doi.org/10.1002/joc.4156

Hartmann D, Klein Tank A, Rusicucci M, Alexander L, Broenniman B, Charabi Y, Dentener F, Dlugokencky E, Easterling D, Kaplan A (2013) Observations: atmosphere and surface. In: Climate change 2013: the physical science basis, contribution of working group I to the fifth assessment report of the intergovernmental panel on climate change. Cambridge University Press, Cambridge, pp 159–254. https://doi.org/10.1017/CBO9781107415324.008

Heistermann M, Crisologo I, Abon CC, Racoma BA, Jacobi S, Servando NT, David CPC, Bronstert A (2013) Brief communication "Using the new Philippine radar network to reconstruct the Habagat of August 2012 monsoon event around Metropolitan Manila". Nat Hazards Earth Syst Sci 13(3):653–657. https://doi.org/10.5194/nhess-13-653-2013

Imaizumi F, Sidle RC, Togari-Ohta A, Shimamura M (2015) Temporal and spatial variation of infilling processes in a landslide scar in a steep mountainous region, Japan: Infilling Process in a Landslide Scar in a Steep Region. Earth Surf Process Landf 40(5):642–653. https://doi.org/10.1002/esp.3659

Jha SK, Zhao H, Woldemeskel FM, Sivakumar B (2015) Network theory and spatial rainfall connections: an interpretation. J Hydrol 527:13–19. https://doi.org/10.1016/j.jhydrol.2015.04.035

Kanae S, Oki T, Kashida A (2004) Changes in hourly heavy precipitation at Tokyo from 1890 to 1999. J Meteorol Soc Jpn 82(1):241–247. https://doi.org/10.2151/jmsj.82.241

Kim JH, Ho CH, Lee MH, Jeong JH, Chen D (2006) Large increase in heavy rainfall associated with tropical cyclone landfalls in Korea after the late 1970s: heavy rainfall and tropical cyclones in Korea. Geophys Res Lett 33(18):L18706. https://doi.org/10.1029/2006GL027430

Knutson TR, McBride JL, Chan J, Emanuel K, Holland G, Landsea C, Held I, Kossin JP, Srivastava AK, Sugi M (2010) Tropical cyclones and climate change. Nat Geosci 3(3):157–163. https://doi.org/10.1038/ngeo779

Krishnan R, Sugi M (2001) Baiu rainfall variability and associated monsoon teleconnections. J Meteorol Soc Jpn 79(3):851–860. https://doi.org/10.2151/jmsj.79.851

Laing A, Evans JL (2015) Global circulation. In: Introduction to tropical meteorology, Chap 3, 2nd edn. COMET. https://www.meted.ucar.edu/sign_in.php?go_back_to=/tropical/textbook/

Lind P, Lindstedt D, Kjellström E, Jones C (2016) Spatial and temporal characteristics of summer precipitation over central Europe in a suite of high-resolution climate models. J Clim 29(10):3501–3518. https://doi.org/10.1175/JCLI-D-15-0463.1

Malik N, Marwan N, Kurths J (2010) Spatial structures and directionalities in monsoonal precipitation over South Asia. Nonlinear Process Geophys 17(5):371–381. https://doi.org/10.5194/npg-17-371-2010

Malik N, Bookhagen B, Marwan N, Kurths J (2012) Analysis of spatial and temporal extreme monsoonal rainfall over South Asia using complex networks. Clim Dyn 39(3–4):971–987. https://doi.org/10.1007/s00382-011-1156-4

Malik N, Bookhagen B, Mucha PJ (2016) Spatiotemporal patterns and trends of Indian monsoonal rainfall extremes: SPATIOTEMPORAL PATTERNS AND TRENDS. Geophys Res Lett 43(4):1710–1717. https://doi.org/10.1002/2016GL067841

Maloney ED, Hartmann DL (2001) The Madden-Julian oscillation, barotropic dynamics, and North Pacific tropical cyclone formation. Part I: observations. J Atmos Sci 58(17):2545–2558. https://doi.org/10.1175/1520-0469(2001)058<2545:TMJOBD>2.0.CO;2

Manda A, Nakamura H, Asano N, Iizuka S, Miyama T, Moteki Q, Yoshioka MK, Nishii K, Miyasaka T (2014) Impacts of a warming marginal sea on torrential rainfall organized under the Asian summer monsoon. Sci Rep. https://doi.org/10.1038/srep05741

Matsumoto J (1989) Heavy rainfalls over East Asia. Int J Climatol 9(4):407–423. https://doi.org/10.1002/joc.3370090407

Monaghan AJ, Rife DL, Pinto JO, Davis CA, Hannan JR (2010) Global precipitation extremes associated with diurnally varying low-level jets. J Clim 23(19):5065–5084. https://doi.org/10.1175/2010JCLI3515.1

Murakami H, Wang B, Kitoh A (2011) Future change of western north pacific typhoons: projections by a 20-km-mesh global atmospheric model. J Clim 24(4):1154–1169. https://doi.org/10.1175/2010JCLI3723.1

Nakazawa T (2006) Madden–Julian oscillation activity and typhoon landfall on Japan in 2004. SOLA 2:136–139. https://doi.org/10.2151/sola.2006-035

Newman MEJ (2010) Networks: an introduction. Oxford University Press, Oxford, New York (**oCLC: ocn456837194**)

Ninomiya K, Akiyama T (1992) Multi-scale features of Baiu, the summer monsoon over Japan and the East Asia. J Meteorol Soc Jpn Ser II 70(1B):467–495. https://doi.org/10.2151/jmsj1965.70.1B_467

Ninomiya K, Muraki H (1986) Large-scale circulations over east asia during Baiu period of 1979. J Meteorol Soc Jpn Ser II 64(3):409–429. https://doi.org/10.2151/jmsj1965.64.3_409

Ninomiya K, Shibagaki Y (2007) Multi-scale features of the Meiyu–Baiu front and associated precipitation systems. J Meteorol Soc Jpn 85B:103–122. https://doi.org/10.2151/jmsj.85B.103

Ninomiya R (1984) Characteristics of Baiu front as a predominant subtropical front in the summer northern hemisphere. J Meteorol Soc Jpn 62(6):880–894

Okada Y, Yamazaki K (2012) Climatological evolution of the Okinawa Baiu and differences in large-scale features during May and June. J Clim 25(18):6287–6303. https://doi.org/10.1175/JCLI-D-11-00631.1

Ozturk U, Marwan N, Korup O, Saito H, Agarwal A, Grossman MJ, Zaiki M, Kurths J (2018) Complex networks for tracking extreme rainfall during typhoons. Chaos Interdiscip J Nonlinear Sci 28(7):075301. https://doi.org/10.1063/1.5004480

Quiroga RQ, Kreuz T, Grassberger P (2002) Event synchronization: a simple and fast method to measure synchronicity and time delay patterns. Phys Rev E. https://doi.org/10.1103/PhysRevE.66.041904

Rheinwalt A, Marwan N, Kurths J, Werner P, Gerstengarbe FW (2012) Boundary effects in network measures of spatially embedded networks. EPL (Europhys Lett) 100(2):28,002. https://doi.org/10.1209/0295-5075/100/28002

Sabidussi G (1966) The centrality index of a graph. Psychometrika 31(4):581–603. https://doi.org/10.1007/BF02289527

Saito H, Nakayama D, Matsuyama H (2010) Relationship between the initiation of a shallow landslide and rainfall intensityduration thresholds in Japan. Geomorphology 118(1–2):167–175. https://doi.org/10.1016/j.geomorph.2009.12.016

Sampe T, Xie SP (2010) Large-scale dynamics of the Meiyu–Baiu rainband: environmental forcing by the westerly jet. J Clim 23(1):113–134. https://doi.org/10.1175/2009JCLI3128.1

Sato T (2013) Mechanism of orographic precipitation around the Meghalaya Plateau associated with intraseasonal oscillation and

the Diurnal cycle. Mon Weather Rev 141(7):2451–2466. https://doi.org/10.1175/MWR-D-12-00321.1

Schieber TA, Carpi L, Díaz-Guilera A, Pardalos PM, Masoller C, Ravetti MG (2017) Quantification of network structural dissimilarities. Nat Commun 8(13):928. https://doi.org/10.1038/ncomms13928

Shimazu Y (1998) Classification of precipitation systems in mature and early weakening stages of typhoons around Japan. J Meteorol Soc Jpn Ser II 76(3):437–445. https://doi.org/10.2151/jmsj1965.76.3_437

Stolbova V, Martin P, Bookhagen B, Marwan N, Kurths J (2014) Topology and seasonal evolution of the network of extreme precipitation over the Indian subcontinent and Sri Lanka. Nonlinear Process Geophys 21(4):901–917. https://doi.org/10.5194/npg-21-901-2014

Stolbova V, Surovyatkina E, Bookhagen B, Kurths J (2016) Tipping elements of the Indian monsoon: prediction of onset and withdrawal: tipping elements of monsoon. Geophys Res Lett 43(8):3982–3990. https://doi.org/10.1002/2016GL068392

Suda K, Asakura T (1955) A study on the unusual "Baiu" season in 1954 by means of northern hemisphere upper air mean charts. J Meteorol Soc Jpn Ser II 33(6):233–244. https://doi.org/10.2151/jmsj1923.33.6_233

TRMM (2011) TRMM (TMPA) rainfall estimate L3 3 hour 0.25 degree x 0.25 degree V7. Goddard Earth Sciences Data and Information Services Center (GES DISC), Greenbelt, MD. https://doi.org/10.5067/TRMM/TMPA/3H/7. Accessed 24 Feb 2016

Tsonis AA, Swanson KL (2008) Topology and predictability of El Niño and La Niña networks. Phys Rev Lett. https://doi.org/10.1103/PhysRevLett.100.228502

Tsonis AA, Swanson KL, Roebber PJ (2006) What do networks have to do with climate? Bull Am Meteorol Soc 87(5):585–595. https://doi.org/10.1175/BAMS-87-5-585

Watts DJ, Strogatz SH (1998) Collective dynamics of 'small-world' networks. Nature 393(6684):440–442. https://doi.org/10.1038/30918

Webster PJ (2005) Changes in tropical cyclone number, duration, and intensity in a warming environment. Science 309(5742):1844–1846. https://doi.org/10.1126/science.1116448

Westra S, Fowler HJ, Evans JP, Alexander LV, Berg P, Johnson F, Kendon EJ, Lenderink G, Roberts NM (2014) Future changes to the intensity and frequency of short-duration extreme rainfall: future intensity of sub-daily rainfall. Rev Geophys 52(3):522–555. https://doi.org/10.1002/2014RG000464

Wolf F, Kirsch C, Donner RV (2019) Edge directionality properties in complex spherical networks. Phys Rev E 99(1):012301. https://doi.org/10.1103/PhysRevE.99.012301

Wu L, Wang B, Geng S (2005) Growing typhoon influence on east Asia: growing typhoon influence on east asia. Geophys Res Lett 32(18):L18703. https://doi.org/10.1029/2005GL022937